Robust Direction of Arrival Estimation in the Presence of Array Faults using Snapshot Diversity

Gary C. F. Lee
Electrical Engineering & Computer Science
Massachusetts Institute of Technology
Cambridge, MA, USA
glcf411@mit.edu

Ankit S. Rawat
Google Research
New York, NY, USA
ankitsrawat@google.com

Gregory W. Wornell
Electrical Engineering & Computer Science
Massachusetts Institute of Technology
Cambridge, MA, USA
gww@mit.edu

***Abstract*—Many direction-of-arrival (DOA) estimation algorithms require accurate measurements from all sensing elements on an antenna array. However, in various practical settings, it becomes imperative to perform DOA estimation even in the presence of faulty elements. In this work, we develop an algorithm that can jointly estimate the DOA of sources and the locations of the faulty elements. This is achieved by introducing weights that describe the degree of *outlierness* of each element. Further, for situations where only single snapshots are available, we propose a new *snapshot diversity* formulation for which our algorithm can still be applied. Simulation results over four different fault models demonstrate that the proposed algorithm robustly estimates DOAs and accurately identifies the faulty elements.**

I. Introduction

Direction-of-arrival (DOA) estimation, an important and well-studied problem in array signal processing, has many applications in wireless communications [1], [2], radar [3]–[5], and sonar [6], [7]. Many DOA estimation algorithms have been proposed in the past decades, including subspace methods, e.g. multiple signal classification (MUSIC) [8], and direct data domain methods, e.g. matrix pencil method [9]. Recently, new techniques based on sparse signal recovery have been proposed [10]–[12]; these methods can be applied even when only a single snapshot is available, or when sources are highly correlated. Nonetheless, the aforementioned methods require accurate signal measurements.

In DOA estimation, several antenna elements are collectively used as a single antenna array to perform the estimation task. Failure of a few elements may arise in practice, which would result in inaccurate estimation if these faulty measurements are not identified and handled. This becomes challenging in certain applications as constant calibration (testing and repair) of the faulty elements is not practical. Therefore, it becomes critical to leverage the inherent redundancy available in various array geometries [13]–[15]. For example, uniform linear array (ULA) allows for DOA estimation even if some of the elements are removed from the array [16]. Motivated by this observation, previous efforts to enable robust DOA estimation have been presented in a few different ways. Firstly, impaired measurements may be presented as missing or invalid values [17]. Here, the locations of the faulty measurements are known, and estimation algorithms include an interpolation step (e.g. matrix completion) from the remaining fault-free measurements. Secondly, faulty measurements may also be due to impulse noise, which can take on arbitrarily large values. In [18], Dai and So model these as outlier measurements with locations being randomly distributed over different snapshots. Thirdly, outliers may manifest in a fraction of the snapshots collected at the array. Robust Principle Component Analysis methods, which find the low-dimensional subspace that captures the fault-free measurements, are used in such cases [19], [20]. There are also several related works that assumes particular fault behavior (e.g. noise only [21]) or known fault locations and instance when failure occurs (e.g. [22]).

In this work, unreliable measurements arise from the presence of faulty components. This differs from the aforementioned scenarios as the locations of faulty elements are fixed across all snapshots. Moreover, these locations are unknown and not immediately obvious from the measurements. In our approach, we introduce weights for each array element representing its degree of *outlierness*. Thus, the objective is to estimate the DOAs and these weights, which is done through an alternating update method. Further, recognizing that only single snapshots may be available in certain applications [23], [24], we propose a new *snapshot diversity* regime, where we utilize a collection of multiple independent single-snapshot measurements. Our simulations show that such a method is capable of accurately identifying the faulty elements for a wide range of number of sources and faulty elements.

II. Signal Model

A. Modeling Arbitrary Fault Behavior

We consider a ULA with N elements, spaced equally at distance d apart (usually chosen as half-wavelength $\lambda_c/2$). M narrowband sources impinge on the ULA at distinct directions, $\boldsymbol{\theta} = \{\theta_0, \ldots, \theta_{M-1}\}$ (where $\theta_m \in (-\pi/2, \pi/2)$). We assume that M source DOAs $\boldsymbol{\theta}$ form a subset of a finely divided grid of P candidate DOAs in the range $(-\pi/2, \pi/2)$ with $P \gg M$. The matrix $\mathbf{A}$ is the $N \times P$ array manifold matrix, with entries $A_{n,p} = \exp\left(j\frac{2\pi}{\lambda_c} nd \sin\theta_p\right)$, $n \in [N],\ p \in [P]$.

Part of this work was done when A. S. Rawat was with MIT.

This work was supported in part by MIT Lincoln Laboratories. G. C. F. Lee is supported by the National Science Scholarship from the Agency for Science, Technology and Research (A*STAR).

978-1-7281-2723-1/19/$31.00 ©2019 IEEE

Thus, for a single snapshot at time t, the measurements from the N ULA elements are

$$\mathbf{y}(t) = \mathbf{A}\mathbf{s}(t) + \boldsymbol{\varepsilon}(t), \tag{1}$$

where the signal $\mathbf{s}(t) \in \mathbb{C}^P$ is M-sparse with non-zero terms at the indices corresponding to the presence of a source at the respective DOA ($\theta_p \in \boldsymbol{\theta}$).

In the fault-free case, the error terms $\boldsymbol{\varepsilon}(t) \in \mathbb{C}^N$ are assumed to follow the additive white Gaussian noise (AWGN) model with variance σ^2. However, if the n-th element is faulty, the corresponding error $\varepsilon_n(t)$ can take on arbitrarily large values. Hence, the error terms can be expressed as

$$\varepsilon_n(t) \sim \mathcal{CN}(0, \sigma_n^2) \tag{2}$$

$$\sigma_n^2 = \left(\frac{\sigma}{\gamma_n}\right)^2 = \begin{cases} \sigma^2, (\gamma_n = 1) \text{ if element } n \text{ is not faulty,} \\ (\frac{\sigma}{\gamma_n})^2, (0 < \gamma_n < 1) \text{ if element } n \text{ is faulty.} \end{cases}$$

Note that $\gamma_n = 1$ describes a non-faulty element and a very small γ_n corresponds to large measurement errors due to faults. This model is similar to that proposed in [25] and [26] for modeling outliers in measurements. We assume that, among the N elements, no more than $N/2$ of them are faulty.

We need sufficiently large samples of $\varepsilon_n(t)$ (over many snapshots) to get a good estimate of σ_n^2, and subsequently γ_n. Nonetheless, we note that in some situations, only single snapshots may be available [23], [24]. Next, we propose that a collection of independent single snapshots, termed as snapshot diversity, can be used to address this problem.

B. Snapshot Diversity

A common formulation in sparse representation problems is the multiple measurement vector (MMV) model. In the context of DOA estimation, this corresponds to DOAs being constant across all snapshots. However, we note that multiple snapshots of static DOAs may not always be available [23], [24].

Instead, we consider the setting where a collection of many independent single-snapshot measurements is collected, highlighting a rather unexplored notion in the context of DOA estimation. We refer to this as *snapshot diversity*. Each snapshot captures sources from a different set, and possibly different number, of DOAs. Stacking the measurements from (1) across T independent snapshots, we obtain the following expression for the $N \times T$ measurements,

$$\mathbf{Y} = [\mathbf{y}(0), \ldots, \mathbf{y}(T-1)] = \mathbf{A}\mathbf{S} + \boldsymbol{\mathcal{E}} = \mathbf{A}\mathbf{S} + \mathbf{E} + \mathbf{W}. \tag{3}$$

The signal $\mathbf{S}$ is a $P \times T$ element-wise sparse matrix, whereby non-zero indices correspond to the presence of the corresponding DOAs in the respective snapshots. The $N \times T$ measurement error matrix $\boldsymbol{\mathcal{E}}$ encapsulates the AWGN, denoted by $\mathbf{W}$, and the errors due to faults, denoted by the row-sparse matrix $\mathbf{E}$ whose support corresponds to the fault locations.

This formulation can be seen as a generalized version of the MMV setup; in the latter case, $\mathbf{S}$ is also row-sparse (static DOAs correspond to the same non-zero indices across all snapshots). However, algorithms for MMV are not applicable for the formulation in (3), since row sparsity is only enforced on $\mathbf{E}$, but not on $\mathbf{S}$, which corresponds to the DOAs.

Nevertheless, rather than treating each snapshot independently, we propose an algorithm that makes use of the row sparsity of $\mathbf{E}$ and the statistics of $\mathbf{W}$ to identify the faulty elements. The snapshot diversity formulation described here aids in estimating γ_n, as the residual terms (i.e., $r_n(t) = y_n(t) - \mathbf{A}_n\hat{\mathbf{s}}(t)$ for some estimate of the signal $\hat{\mathbf{s}}$) are independently and identically distributed for the same n, regardless of the underlying DOAs for each snapshot.

In the next section, we leverage the setup with snapshot diversity described here and propose an algorithm that identifies the faulty elements and estimates DOAs through alternating updates.

III. Algorithm

A. Weighted Sparse Signal Recovery

Given the observations $\mathbf{Y}$ in our model setup (cf. (2) and (3)), we are interested in estimating the nonnegative outlier weights $\boldsymbol{\gamma} = [\gamma_1, \gamma_2, \ldots, \gamma_N]$ and the DOAs $\boldsymbol{\theta}$ from the non-zero indices of the signal $\mathbf{S}$ that minimizes the weighted residual $\|\text{diag}(\boldsymbol{\gamma}) \cdot (\mathbf{Y} - \mathbf{A}\mathbf{S})\|_F^2$. Recall that sparsity conditions are imposed on $\mathbf{S}$ and on the number of faulty elements present. The latter conditions translates to $\gamma_n < 1$ for as few elements as possible. Therefore, our overall objective function can be stated as follows

$$\arg\min_{\mathbf{S},\boldsymbol{\gamma}} \|\text{diag}(\boldsymbol{\gamma}) \cdot (\mathbf{Y} - \mathbf{A}\mathbf{S})\|_F^2 + \alpha\|\mathbf{S}\|_0 + \lambda\|\log(\boldsymbol{\gamma})\|_1. \tag{4}$$

Note that $\|\mathbf{S}\|_0$ and $\|\log(\boldsymbol{\gamma})\|_1$ encapsulate the aforementioned sparsity conditions of the problem. In particular, the ℓ_1 term over $\log(\boldsymbol{\gamma})$ is based on a similar model proposed by [25], and corresponds to an inverse power prior distribution on the outlier weights.

B. Alternating Method of DOA and Outlier Estimation

Note that (4) describes a non-convex optimization problem. However, when $\mathbf{S}$ is fixed, the objective becomes convex in $\boldsymbol{\gamma}$; on the other hand, for a fixed $\boldsymbol{\gamma}$, the problem outlines a typical sparse signal recovery problem [12], [27]. In line with similar problems, we propose an iterative algorithm that performs alternating updates on $\boldsymbol{\gamma}$ and $\mathbf{S}$ (cf. Algorithm 1).

The main computation in each iteration of Algorithm 1 lies in the DOA estimation ($\mathbf{S}$) for fixed $\boldsymbol{\gamma}$. We adopt a variant of orthogonal matching pursuit (OMP) – weighted OMP (W-OMP) [26] – which has low computational and time complexity [28]. Upon fixing $\mathbf{S}$, the outlier weights γ_n can be estimated from the residuals. Inspecting (4) when λ and $\mathbf{S}$ are fixed, $\boldsymbol{\gamma}$ takes a closed form, where for each $n \in [N]$,

$$\gamma_n^* = \sqrt{\frac{\lambda/T}{\frac{2}{T}\sum_{t=1}^{T}\left(y_n(t) - \mathbf{A}_n\mathbf{s}(t)\right)^2}} = \frac{\sqrt{\frac{\lambda}{2T}}}{\widehat{\sigma}_n} = \frac{\widehat{\sigma}_{\text{ref}}}{\widehat{\sigma}_n}. \tag{5}$$

The update step for γ_n at each iteration can be seen as a ratio of a reference term ($\widehat{\sigma}_{\text{ref}}$) and the second raw moment of the residuals (which also corresponds to the standard deviation, $\widehat{\sigma}_n$, following the zero-mean assumption about the errors).

Algorithm 1 Alternating Method for Determining DOAs and Outlier Weights under Snapshot Diversity

Input: $\mathbf{Y} = [\mathbf{y}(0), \ldots, \mathbf{y}(T-1)]$
Output: $\widehat{\boldsymbol{\gamma}} = [\widehat{\gamma}_1, \ldots, \widehat{\gamma}_N]$, $\widehat{\mathbf{S}} = [\hat{\mathbf{s}}(0), \ldots, \hat{\mathbf{s}}(T-1)]$

Initialization: Set all $\gamma_n = 1$, $\forall n \in [N]$
for $i = 1$ to i_{max} **do**
  for all snapshots $t = 0$ to $T-1$ **do**
    Estimate $\hat{\mathbf{s}}^{(i)}(t)$ and $\hat{\mathbf{e}}^{(i)}(t)$ using weighted OMP
    Residual $\mathbf{r}^{(i)}(t) = \mathbf{y}(t) - \mathbf{A}\hat{\mathbf{s}}^{(i)}(t)$
  end for
  Estimate $\widehat{\boldsymbol{\gamma}}^{(i)}$ from residuals $\mathbf{R}^{(i)}$ using Algorithm 2
  if $\|\widehat{\boldsymbol{\gamma}}^{(i)} - \widehat{\boldsymbol{\gamma}}^{(i-1)}\| < \epsilon$ **then**
    BREAK
  end if
end for
return $\widehat{\boldsymbol{\gamma}}^{(i)}$, $\widehat{\mathbf{S}}^{(i)}$

Note that we also need to impose an additional clipping step to ensure γ_n is constrained to the interval $[0, 1]$.

The above expression reflects the effect of Lagrange parameter λ on the estimation of the weights γ_n – a large λ leads to more γ_n terms getting clipped to 1, and would therefore be less sensitive to outliers. On the other hand, a small λ promotes all γ_n terms to be small, but this may induce false positives (i.e., implying that the element is faulty even if it is not).

In Algorithm 1, the W-OMP algorithm [26] solves for (3) to jointly estimate $\mathbf{S}$ and $\mathbf{E}$, although the latter term is not used in the subsequent step. This is achieved by appending an $N \times N$ identity matrix to the array manifold matrix $\mathbf{A}$, forming an expanded dictionary for the sparse signal recovery. The use of this expanded dictionary to account for $\mathbf{E}$ is believed to aid in faster convergence, since it can capture the large magnitude errors, and can reduce DOA estimation errors when estimating $\mathbf{S}$ in the presence of large faults in the earlier iterations.

After obtaining the outlier weights $\boldsymbol{\gamma}$ from Algorithm 1, a final round of DOA estimation can be performed with W-OMP without the identity matrix (i.e., only estimating $\mathbf{S}$), since the errors due to faulty elements have been accounted for through the outlier weights.

C. Estimating Variance and Weights

A key step in Algorithm 1 is estimating γ_n from the residuals. In the context of (2), $\widehat{\sigma}_{\text{ref}}$ is related to the standard deviation of the AWGN. However, as seen in (5), $\widehat{\sigma}_{\text{ref}}$ can be adjusted, in relation to the Lagrange multiplier λ, to tune the sensitivity of the faulty element detection.

Firstly, to obtain a robust estimation of variability of the AWGN, we chose the median absolute deviation (MAD) statistic. The MAD of all the complex residual terms is

$$\text{MAD}(\mathbf{R}) = \sqrt{\text{median}(\text{Re}\{\mathbf{R}\})^2 + \text{median}(\text{Im}\{\mathbf{R}\})^2}, \quad (6)$$

where $\text{Re}\{\mathbf{R}\}$ and $\text{Im}\{\mathbf{R}\}$ refers to the real and imaginary parts of the residuals respectively. Note that $\mathbb{E}[\text{Re}\{\mathbf{R}\}] = \mathbb{E}[\text{Im}\{\mathbf{R}\}] = 0$ since we assume that the distribution of $\mathbf{R}$ is centered about 0.

Algorithm 2 Weight Estimation

Input: $\mathbf{R} = [\mathbf{r}(0), \ldots, \mathbf{r}(T-1)]$
Output: $\widehat{\boldsymbol{\gamma}} = [\widehat{\gamma}_1, \ldots, \widehat{\gamma}_N]$

for $n = 1$ to N **do**
  $\widehat{\sigma}_n = \sqrt{\mathbb{E}_t\left[|r_n(t)|^2\right]} = \sqrt{\frac{1}{T}\left(\mathbf{r_n}\mathbf{r_n^H}\right)}$
  (under the assumption that $\mathbb{E}_t\left[r_n(t)\right] = 0$)
end for
Compute reference term from median absolute deviation $\widehat{\sigma}_{\text{ref}} = k \cdot \text{MAD}(\mathbf{R})$, (with chosen parameter: $k = 10$)
Weight Estimation: $\gamma_n = \min\left(\frac{\widehat{\sigma}_{\text{ref}}}{\widehat{\sigma}_n}, 1\right)$, $\forall n \in [N]$
return $\widehat{\boldsymbol{\gamma}}$

Subsequently, we obtain an estimate of the reference value

$$\widehat{\sigma}_{\text{ref}} = k \cdot \text{MAD}(\mathbf{R}).$$

For a Gaussian distribution, [29] describes using $k = 1.4826$ to attain the standard deviation. However, in the context of Algorithm 2, the value of k is associated with the Lagrange multiplier λ and serves as a hyperparameter.

Remark. *The choice of a small k corresponds to a small λ, which in turn favors small γ_n estimates but may result in false positives in fault detection. On the other hand, a significantly large k favors large γ_n estimates, and result in less sensitive fault detection.*

The choice of $k = 10$ was empirically found to be the most effective across several fault models studied in our simulations.

IV. Simulation Results

In this section, we empirically evaluate the proposed algorithm. We conduct Monte Carlo simulations of a ULA ($N = 32$) under different conditions. For each trial, we generate 100 snapshots, each with different number of DOAs (between 1 and 8), randomly generated from a sufficiently fine grid ($\theta_m \in (-70°, 70°)$ to avoid DOAs near the array endfires). We enforce a minimum separation on the DOAs (i.e., for two sources θ and θ', $|\sin\theta - \sin\theta'| > 4/(N-1)$), a necessary condition for parameter identifiability in a mixture of sines and spikes [30].

To simulate faulty elements, we explore four fault behaviors – zeroed measurements (cf. (7a)), random measurements (cf. (7b)), measurements with higher noise variance (cf. (7c)) and off-position model mismatch (cf. (7d)).

$$y_{n,\text{faulty}} = 0 \quad (7a)$$

$$y_{n,\text{faulty}} \sim \mathcal{CN}(0, M) \quad (7b)$$

$$y_{n,\text{faulty}} \sim \mathcal{CN}(y_{n,\text{true}}, \sigma^2_{\text{10dB SNR}}) \quad (7c)$$

$$y_{n,\text{faulty}} = \sum_{m=0}^{M-1} s_m \exp((n+\delta) j\omega_m) \quad (7d)$$

$$\delta \in \{[-0.75, -0.25] \cup [0.25, 0.75]\}$$

The default signal-to-noise ratio (SNR) is 30 dB. For each test case, we conduct 100 independent trials, and the results are reported below.

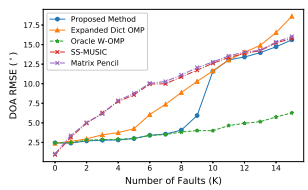

(7a) Zeroed Measurements

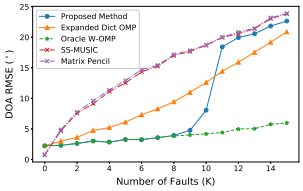

(7b) Random Measurements

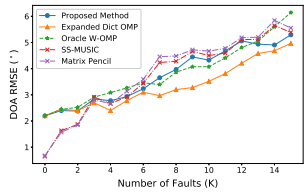

(7c) Noisy (10dB) Measurements

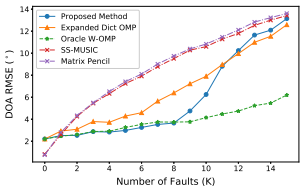

(7d) Position Model Mismatch

Fig. 1. Plot of average RMSE of DOAs (in degrees) across 100 trials under 4 different fault conditions ((7a) – (7d))

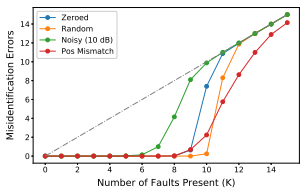

(a)

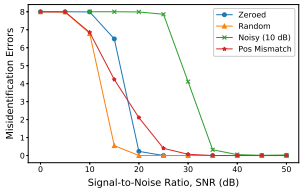

(b)

Fig. 2. Plot of errors in identifying faulty and non-faulty elements against (a) number of faulty elements present (at 30 dB SNR) and (b) the measurements' SNR (with 8 faults present) for the 4 respective fault conditions simulated. The gray dotted line corresponds to the number of faulty elements present.

A. DOA Estimation

To study the performance of the DOA estimation, we used the following root-mean-square error (RMSE) metric,

$$RMSE(\widehat{\boldsymbol{\theta}},\boldsymbol{\theta}) = \sqrt{\frac{1}{100}\sum_{z=1}^{100}\frac{1}{T}\sum_{t=0}^{T-1}\frac{1}{M(t)}\sum_{m=0}^{M(t)-1}\left(\widehat{\theta}_m(t)-\theta_m(t)\right)^2} \quad (8)$$

where $M(t)$ is the number of sources for the t-th snapshot. We assume that the number of sources are known; i.e., the algorithms obtain the best M DOA estimates. (In rare cases where less than M DOAs are estimated, the snapshot is omitted from the RMSE calculation.)

We benchmarked the performance of our algorithm against two conventional single-snapshot algorithms (with no correction for faults) – single snapshot MUSIC [31] and matrix pencil [9]. We also provide the performance of the DOAs estimated through a single iteration of the expanded dictionary OMP, and through OMP with "oracle weights" (i.e., $\gamma_n = 1$ for non-faulty elements, and $\gamma_n = 0$ for faulty elements).

The DOA RMSE obtained from these algorithms were compared for the four fault models studied (Figure 1). In three out of the four fault models, our proposed algorithm consistently obtains lower RMSE compared to MUSIC and matrix pencil methods when only 1 to 8 faulty elements are present, but performs equally poorly when more than 8 faults are present. Under (7c), the algorithms have very similar performance. We believe that this reflects the robustness of the algorithms studied, and in particular SS-MUSIC and matrix pencil, against low SNR (i.e., high variance AWGN). Therefore, the DOA estimation was not impacted significantly in both the conventional methods and in our proposed algorithm.

B. Fault Detection

To assess the fault detection performance, we classify elements with final weights below a set threshold (e.g. $\gamma_n < 1$) as faulty. Subsequently, we compare the errors in identifying the elements (both missed detection of faulty elements and false alarms on non-faulty elements). Changing the threshold affects the sensitivity level of detection/false alarm. In our simulations, it was found that up to 6 faulty elements can be accurately identified under the snapshot diversity condition with our proposed algorithm (Figure 2(a)).

We also investigated the detection of 8 faulty elements at various SNR of the measurements (Figure 2(b)). Our algorithm performs well in identifying the 8 faulty elements under high SNR regime. However, as observed in (7c), the algorithm deteriorates even at 30 dB SNR. Under this fault model, both the fault errors and the measurement noise follow a Gaussian distribution but with slightly different variance. As the variance of the fault errors approaches that of the measurement noise, the distinction between the faulty and non-faulty measurements become less discernible. In such situations, choosing a smaller factor k may help in accentuating the distinction between fault and noise and help increase sensitivity in fault detection.

C. Discussion

In our setup, we model faults as arbitrary additive terms, i.e., we do not consider signal dependent noise or interference. We hope to expand our analysis and experiments to consider these factors in future works. Further, we recognize that our algorithm depends on the difference in magnitude of the variance between the measurement AWGN and the fault errors. Future directions include a more well-informed choice of factor k or estimation of the $\boldsymbol{\gamma}$ vector.

It should also be highlighted that the estimation of the signal $\mathbf{S}$ in the alternating steps is an approximation to the original sparse recovery problem. The suboptimal estimation of $\mathbf{S}$ was counteracted by an overestimate over the measurement error through a larger $\widehat{\sigma}_{\text{ref}}$. Refinement to this estimation in the iterative alternating step could be explored.

V. Conclusion

In this work, we develop a framework to identify faulty elements on a ULA through outlier weights. This helps us develop an alternating update method to robustly estimate DOAs from unreliable measurements generated by the array. Utilizing a novel concept of snapshot diversity, the proposed method also applies to the settings where only a single snapshot is available. The empirical evaluation of the proposed method under four different fault model demonstrates its efficacy.

REFERENCES

[1] L. C. Godara, "Application of antenna arrays to mobile communications, part II: Beam-forming and direction-of-arrival considerations," *Proceedings of the IEEE*, vol. 85, no. 8, pp. 1195–1245, 1997.

[2] M. H. Haroun, M. Cabedo-Fabres, H. Ayad, J. Jomaah, and M. Ferrando-Bataller, "Direction of arrival estimation for LTE-advanced and 5G in the uplink," in *2018 IEEE Middle East and North Africa Communications Conference (MENACOMM)*. IEEE, Apr 2018, pp. 1–6.

[3] X. Guo and H. Sun, "Compressive sensing for target DOA estimation in radar," in *2014 International Radar Conference*. IEEE, Oct 2014, pp. 1–5.

[4] M. Greco, F. Gini, A. Farina, and L. Timmoneri, "Direction-of-arrival estimation in radar systems: moving window against approximate maximum likelihood estimator," *IET Radar, Sonar & Navigation*, vol. 3, no. 5, pp. 552–557, 2009.

[5] S. Cho, H. Song, K. You, and H. Shin, "A new direction-of-arrival estimation method using automotive radar sensor arrays," *International Journal of Distributed Sensor Networks*, vol. 13, no. 6, Jun 2017.

[6] R. Rajagopal and P. Rao, "Generalised algorithm for DOA estimation in a passive sonar," *IEE Proceedings F Radar and Signal Processing*, vol. 140, no. 1, pp. 12–20, 1993.

[7] H. Zhang, F. Zhang, M. Chen, and H. Fu, "Non-uniform linear sonar array based DOA estimation," in *Proceedings of the 33rd Chinese Control Conference*. IEEE, Jul 2014, pp. 7240–7243.

[8] R. Schmidt, "Multiple emitter location and signal parameter estimation," *IEEE Transactions on Antennas and Propagation*, vol. 34, no. 3, pp. 276–280, Mar 1986.

[9] Y. Hua and T. K. Sarkar, "Matrix pencil method for estimating parameters of exponentially damped/undamped sinusoids in noise," *IEEE Transactions on Acoustics, Speech, and Signal Processing*, vol. 38, no. 5, pp. 814–824, May 1990.

[10] D. Malioutov, M. Cetin, and A. Willsky, "A sparse signal reconstruction perspective for source localization with sensor arrays," *IEEE Transactions on Signal Processing*, vol. 53, no. 8, pp. 3010–3022, Aug 2005.

[11] N. Hu, Z. Ye, X. Xu, and M. Bao, "DOA estimation for sparse array via sparse signal reconstruction," *IEEE Transactions on Aerospace and Electronic Systems*, vol. 49, no. 2, pp. 760–773, Apr 2013.

[12] Z. Yang, J. Li, P. Stoica, and L. Xie, "Sparse methods for direction-of-arrival estimation," in *Academic Press Library in Signal Processing, Volume 7*. Elsevier, 2018, pp. 509–581.

[13] A. Moffet, "Minimum-redundancy linear arrays," *IEEE Transactions on Antennas and Propagation*, vol. 16, no. 2, pp. 172–175, Mar 1968.

[14] V. Lefkaditis and A. Manikas, "Investigation of sensor failure with respect to ambiguities in linear arrays," *Electronics Letters*, vol. 35, no. I, pp. 22–23, 1999.

[15] C. Zhu, W. Wang, H. Chen, and H. So, "Impaired sensor diagnosis, beamforming, and DOA estimation with difference co-array processing," *IEEE Sensors Journal*, vol. 15, no. 7, pp. 3773–3780, 2015.

[16] C.-L. Liu and P. P. Vaidyanathan, "Robustness of coarrays of sparse arrays to sensor failures," *2018 IEEE International Conference on Acoustics, Speech and Signal Processing (ICASSP)*, no. 1, pp. 3231–3235, 2018.

[17] T. Yerriswamy and J. S.N., "Fault tolerant matrix pencil method for direction of arrival estimation," *Signal & Image Processing : An International Journal*, vol. 2, no. 3, pp. 55–67, Sep 2011.

[18] J. Dai and H. So, "Sparse bayesian learning approach for outlier-resistant direction-of-arrival estimation," *IEEE Transactions on Signal Processing*, vol. 66, no. 3, pp. 744–756, 2018.

[19] H. Xu, C. Caramanis, and S. Mannor, "Outlier-robust PCA: The high-dimensional case," *IEEE Transactions on Information Theory*, vol. 59, no. 1, pp. 546–572, 2013.

[20] C. Chenot and J. Bobin, "Blind separation of sparse sources in the presence of outliers," *Signal Processing*, vol. 138, pp. 233–243, 2017.

[21] S. Vigneshwaran, N. Sundararajan, and P. Saratchandran, "Direction of arrival (DoA) estimation under array sensor failures using a minimal resource allocation neural network," vol. 55, no. 2, pp. 334–343, 2007.

[22] E. Larsson and S. P., "High-resolution direction finding: the missing data case," *IEEE Transactions on Signal Processing*, vol. 49, no. 5, pp. 950–958, May 2001.

[23] P. Häcker and B. Yang, "Single snapshot DOA estimation," *Advances in Radio Science*, vol. 8, pp. 251–256, Oct 2010.

[24] C. Degen, "On single snapshot direction-of-arrival estimation," in *2017 IEEE International Conference on Wireless for Space and Extreme Environments (WiSEE)*, no. 4. IEEE, Oct 2017, pp. 92–97.

[25] X. Gao and Y. Fang, "Penalized Weighted Least Squares for Outlier Detection and Robust Regression," Mar 2016. [Online]. Available: http://arxiv.org/abs/1603.07427

[26] L. Liu, L. Chen, C. Chen, Y. Tang, and C. Pun, "Weighted joint sparse representation for removing mixed noise in image," *IEEE Transactions on Cybernetics*, vol. 47, no. 3, pp. 600–611, 2017.

[27] Q. Shen, W. Liu, W. Cui, and S. Wu, "Underdetermined DOA estimation under the compressive sensing framework: A review," *IEEE Access*, vol. 4, pp. 8865–8878, 2016.

[28] A. Aich and P. Palanisamy, "On application of OMP and CoSaMP algorithms for DOA estimation problem," in *2017 International Conference on Communication and Signal Processing (ICCSP)*, April 2017, pp. 1983–1987.

[29] P. J. Rousseeuw and C. Croux, "Alternatives to the median absolute deviation," *Journal of the American Statistical Association*, vol. 88, no. 424, pp. 1273–1283, 1993.

[30] C. Fernandez-Granda, G. Tang, X. Wang, and L. Zheng, "Demixing sines and spikes: Robust spectral super-resolution in the presence of outliers," *Information and Inference: A Journal of the IMA*, vol. 7, no. 1, pp. 105–168, Mar 2018.

[31] W. Liao and A. Fannjiang, "MUSIC for single-snapshot spectral estimation: Stability and super-resolution," *Applied and Computational Harmonic Analysis*, vol. 40, no. 1, pp. 33–67, Jan 2016.